2D IMAGE RECONSTRUCTION USING NATURAL NEIGHBOUR INTERPOLATION

François Anton ♭, Darka Mioc ♮ and Alain Fournier ♭

♭Department of Computer Science
University of British Columbia
203-2366 Main Mall, Vancouver, BC, V6T 1Z4, Canada
fanton,fournier@cs.ubc.ca
♮Département des Sciences Géomatiques
Université Laval
Pavillon Casault, Ste-Foy, QC, G1K 7P4, Canada
dmioc@cs.ubc.ca

ABSTRACT

In this paper, we explore image reconstruction from irregularly spaced samples using natural neighbour interpolation. We sample the image irregularly using techniques based on the Laplacian or the derivative in the direction of the gradient. Local coordinates based on the Voronoi diagram are used in natural neighbour interpolation to quantify the "neighbourliness" of data sites. Then we use natural neighbour interpolation in order to reconstruct the image. The main result is that the image quality is always very good in the case of the sampling techniques based on the Laplacian.

Keywords: image reconstruction, irregularly spaced samples, natural neighbour interpolation, local coordinates

1 INTRODUCTION

In this paper, we explore image reconstruction using natural neighbour interpolation. This implies sampling the image irregularly, and then applying the natural neighbour interpolation. In our case, the interpolant is the level of gray, since we will apply sampling and reconstruction on black and white images. Spatial interpolation has been used in Computer Graphics, in order to generate intermediate images in animation (also called "inbetweening", see [Foley90]), or in 3D visual models reconstruction [Kuo98], or in order to reconstruct radiosity over a patch [Hinke98]. In spatial interpolation, local techniques have been used in order to get an interpolation continuous at data points, and smooth around data points. In these local techniques, the data points which influence the interpolant are the ones neighbouring the given interpolation point. The interpolation is thus based on the definition of adjacency or of neighbourliness. In 1D, the neighbourliness is given by the natural topology of the real line, induced by its total order. In

2D, there is no such relationship, and the neighbourliness can be defined by some topological structure. Such structures include the Delaunay triangulation, that is the dual of the Voronoi diagram. The Delaunay triangulation has been extensively used in linear interpolation (which corresponds to convolving with the triangle or Barlett filter [Foley90]). Another local technique is the natural neighbour interpolation [Sibso81] based on local coordinates [Sibso80].

These local coordinates were introduced by Sibson [Sibso80]. Local coordinates based on the Voronoi diagram are used in natural neighbour interpolation (also studied in [Gold94] as "stolen area" interpolation), to quantify the "neighbourliness" of data sites. The properties of these local coordinates have been extensively studied by Sibson [Sibso80] and Piper [Piper93], who gave a formula for the gradient of the volume stolen from neighbouring Voronoi regions due to the insertion of a query point, obtained from two directional derivatives. The natural neighbour or stolen area interpolation technique has been extended from ordinary Voronoi diagrams to Voronoi diagrams for sets of points and line segments in [Anton98]. Anton et *al.* [Anton98] extended the results presented in Gold and Roos [Gold94], by providing direct vectorial formulas for the first order and second order derivatives for the stolen area. The analysis presented in [Anton98] generalizes the analysis of Piper [Piper93] based on the formalism of partial derivatives, to the formalism of derivatives of a function on a normed space.

In section 2, we present three different techniques to sample irregularly an image. In section 3, we present the natural neighbour interpolation technique. In section 4, we present the image reconstruction algorithm that uses the natural neighbour interpolation technique. Finally, in section 5, we present the experimental results of the 2D image reconstruction.

2 THE IRREGULAR SAMPLING

Different kinds of irregular sampling techniques can be used: irregular point sampling, irregular area sampling (unweighted and weighted), importance sampling, stochastic sampling, or adaptive stochastic sampling [Foley90]. Since the derivative of the natural neighbour interpolant we will use for reconstruction is continuous except at data points, it is best to select data points where the variation of the intensity (the quantity to be reconstructed) is highest, therefore the edges in the image. A wide variety of edge detection algorithms exist, but the set of basic tools on which the most general algorithms are built is reduced to differencing: the derivative in the gradient direction, the Laplacian, the directional derivatives and the statistical differencing. We used two edge detection algorithms based on the Laplacian, and one edge detection algorithm based on the derivative in the direction of the gradient, in order to get samples around the high frequency changes in the image. We will present now the three edge detection algorithms that we have used for sampling.

The gradient is the first order differential of the interpolant at the point. The derivative in the direction of the gradient gives the highest variation of the interpolant (in our case the level of gray) at the point. This derivative in the direction of the gradient equals to the highest magnitude of the derivative, i.e. the square root of the sum of the squares of the derivatives in any pair of orthogonal directions, e.g. $\left[\left(\frac{\partial f}{\partial x}\right)^2 + \left(\frac{\partial f}{\partial y}\right)^2\right]^{\frac{1}{2}}$ [Rosen69]. This is a well behaved function used in image sharpening and edge detection, e.g. in the Prewitt and Sobel edge detectors

[Ritte96]. In the gradient based sampling that we used, we took the square root of the sum of the square of the difference between the row above and the row below the pixel, and the square of the difference between the strip on the left and the strip on the right of the pixel.

The Laplacian ($\nabla^2 f = \frac{\partial^2 f}{\partial x^2} + \frac{\partial^2 f}{\partial y^2}$) is proportional to the variation of the derivative of the interpolant at the point with respect to an annulus centered at the point. We used two different computations for the Laplacian, the standard Laplacian, and an alternative Laplacian where the "annulus" is composed of eight pixels instead of four. In this alternative Laplacian, a $\frac{1}{\sqrt{2}}$ factor is used to compensate for the wider diagonal pixel separation. These two Laplacian based sampling techniques are the other two sampling techniques we used in our experimentation.

The sampling consists in selecting all the pixels whose derivative operator value is bigger than some threshold. After the image is irregularly sampled, the Voronoi diagram (and its dual graph: the Delaunay triangulation) of the set of samples is computed using an incremental algorithm based on the Quad-Edge data structure (see Guibas and Stolfi [Guiba85] for an introduction to the Quad-Edge data structure and the algorithms for the construction of the Voronoi diagram based on this data structure).

3 THE NATURAL NEIGHBOUR INTERPOLATION

In this section, we will make a brief introduction to the natural neighbour interpolation work developed by Anton et al. [Anton98]. We have a set $O = \{O_1, ..., O_n\}$ of neighbouring data points, at which we know the value of the interpolant, and we want to interpolate the value of the interpolant at some unknown location M in the convex hull of O. In order to interpolate the value of the interpolant at M from the values at neighbouring data sites, we compute the local coordinates of M.

These local coordinates are defined as follows: $u_k(M) = \frac{\lambda_k(M)}{\sum_i \lambda_i(M)}$, where $\lambda_k(M)$ is the area of the intersection (region marked as V_k on Figure 1) of the "old" tile of O_k and the "new" tile of M.

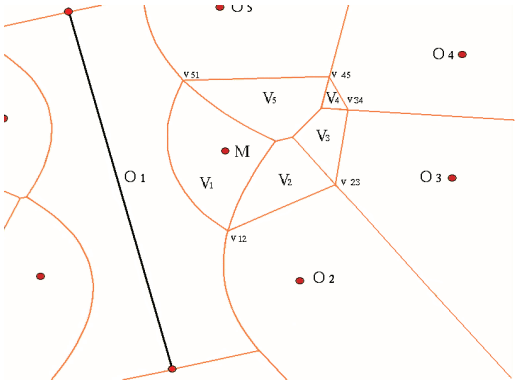

Figure 1: Natural neighbour interpolation

The vectorial expression for the Voronoi vertex (circumcentre) of P_i, P_j, and M is:

$$\overrightarrow{v_{i\,i+1}} = \overrightarrow{m_{i\,i+1}} + \frac{\overrightarrow{P_{i+1}M} \cdot \overrightarrow{P_iM}}{2\overrightarrow{n_{i\,i+1}} \cdot \overrightarrow{P_iM}} \overrightarrow{n_{i\,i+1}},$$

where $m_{i\,i+1}$ is the middle of $[P_iP_{i+1}]$, and $n_{i\,i+1} = \begin{pmatrix} P_{i+1,2} - P_{i,2} \\ P_{i,1} - P_{i+1,1} \end{pmatrix}$.

From this expression, we get that the Voronoi vertex is defined, continuous and differentiable except at data sites, and its derivative at the point M is:

$$D\overrightarrow{v_{i\,i+1}}(M) = \frac{d\overrightarrow{M} \cdot \overrightarrow{v_{i\,i+1}M}}{\overrightarrow{n_{i\,i+1}} \cdot \overrightarrow{O_iM}} \overrightarrow{n_{i,i+1}}.$$

In order to determine $\lambda_k(M)$, we decompose the corresponding area in triangles (see Figure 2): $v_{k-1\,k}$, $v_{k\,k+1}$, $C_{k\,1}$ and $v_{k-1\,k}$, $C_{k\,j}$, $C_{k\,j+1}$, where $C_{k\,j}$ is the i^{th} Voronoi vertex of $V(O_k)$ in the counterclockwise orientation from $\overrightarrow{v_{k-1\,k}v_{k\,k+1}}$ and

we get the following result:

$$2\lambda_k(M) = det\left(\overrightarrow{v_{k-1\,k}v_{k\,k+1}}, \overrightarrow{v_{k-1\,k}C_{k\,1}}\right)$$

$$+\sum_{j=1}^{J_k} det\left(\overrightarrow{v_{k-1\,k}C_{k\,j}}, \overrightarrow{v_{k-1\,k}C_{k\,j+1}}\right).$$

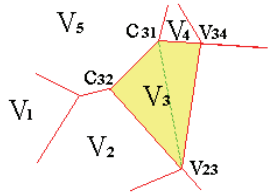

Figure 2: Decomposition into triangles

Therefore, the local coordinates are defined, continuous, and differentiable everywhere except at data sites, and we get:

$$2D\lambda_k(M) = det\left(d\overrightarrow{v_{k-1\,k}}, \overrightarrow{C_{k\,J_k}v_{k\,k+1}}\right) +$$

$$det\left(d\overrightarrow{v_{k\,k+1}}, \overrightarrow{v_{k-1\,k}C_{k\,1}}\right).$$

By the chain rule $D\lambda_k(M) = \nabla\lambda_k(M) \cdot d\overrightarrow{M}$, we get the direct formula for the gradient of the area stolen to O_k by M.

4 THE RECONSTRUCTION

The reconstruction of the image follows the sampling and the construction of the Delaunay triangulation and the Voronoi diagram for the set of samples. The reconstruction is achieved by the natural neighbour interpolation technique. The image is reconstructed by interpolating the gray level of each pixel. In order to interpolate the gray level of a pixel, the algorithm locates an edge of the triangle of the Delaunay triangulation in which the pixel lies. Then, it determines if the pixel is a vertex of the triangle in which it lies. If this is the case, it means that the pixel is one of the samples, and therefore its gray level is the gray level of the sample. If it is not the case, the algorithm computes the list of vertices from which the pixel would steal some area if it was inserted in the Delaunay triangulation. This is done without inserting the pixel in the Delaunay triangulation. Starting from the located edge, and visiting the three edges of the enclosing triangle, the algorithm tests whether the given edge is safe (an edge is not safe if it should be swapped, resulting in a triangle swap by exchange of the common edge of two adjacent triangles [Guiba85]). If an edge is safe, then it is added to the circular list of safe edges enclosing the interpolated pixel. If an edge is not safe, the edge having the same origin and immediately after it in the clockwise orientation (the edge pointed by its Oprev operator [Guiba85]), and the edge having the same destination and immediately after it in the counterclockwise orientation (the edge pointed by its Dnext operator [Guiba85]) are successively checked. The safe edges detected by this algorithm are inserted in a circular list in the counterclockwise order, and the "previous" pointer points to the previous edge in the counterclockwise orientation. The origin of the edge pointed by the Rot operator [Guiba85] of each edge of this circular list is a natural neighbour of the pixel being interpolated.

Once the list of enclosing safe edges is computed, the stolen area by the interpolated point to each associated neighbour and the interpolated gray level are computed and the total area and the sum of interpolated gray levels maintained. Once all the neighbours have been visited, the sum of the interpolated gray levels is divided by the total area in order to get the interpolated value of gray level for the pixel. The construction of the Quad-Edge data structure requires like the Voronoi diagram $O(n\,logn)$ worst case time, where n is the number of sampled pixels. The reconstruction requires $O(N\,logn)$ expected time (like an incremental algorithm for the Voronoi diagram), where N is the number of pixels in the image.

5 EXPERIMENTAL RESULTS

We applied the three sampling techniques in conjunction with the natural neighbour interpolation for reconstructing the images. For the sampling, we set the threshold to 0, such as all the pixels whose floor of the derivative operator value is bigger than 0 are selected.

This corresponds in the case of the Laplacian to selecting the pixels whose gray level differs by at least one from the average of the neighbouring pixels. We analyzed the results of the image reconstruction after each type of sampling using error measures (L_1, L_2, and L_∞ norms), as used in [Hinke98], and the compression ratio (the ratio of the number of unsampled pixels by the size of the image). These numerical results of the reconstruction of images are given for five images in the Tables 1, 2, 3, 4 and 5. The root mean square error is usually considered as an error measure for the quality of the image (with resolution and accutance [Rosen76]). The graphical result of the sampling and the reconstruction for one of the images (blood cells image, see Figure 3) are presented in the Figures 4, 5, 6, 7, 8 and 9. The other original images (goat, bone marrow, figure, mailbox) are shown in the Figures 10, 12, 14 and 16. Due to space limitations, we showed only the best reconstruction (i.e. lowest L_∞) for these images (see Figures 11, 13, 15 and 17).

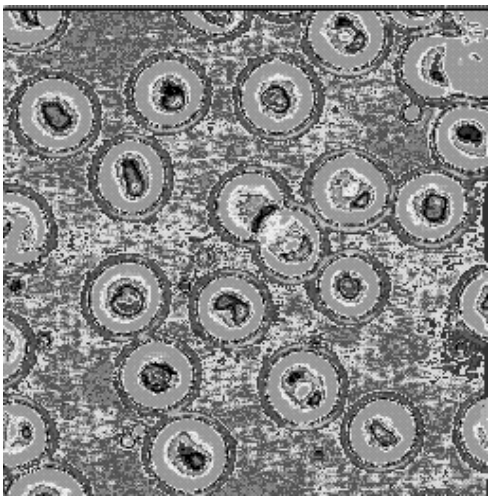

Figure 3: Original image of blood cells

Measures	Lapl.	Grad.	Alt. L.
L_1	0.0248	0.1727	0.3558
L_2	0.2662	3.0881	3.4607
L_∞	26	131	80
Compression	13.1%	0.7%	1.4%

Table 1: Results for blood cells image (Figure 3)

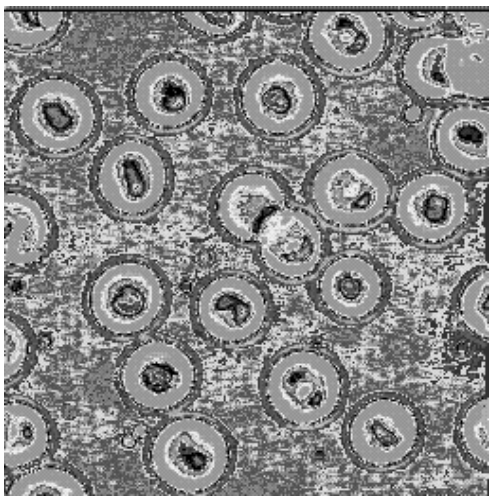

Figure 4: Reconstruction using Laplacian

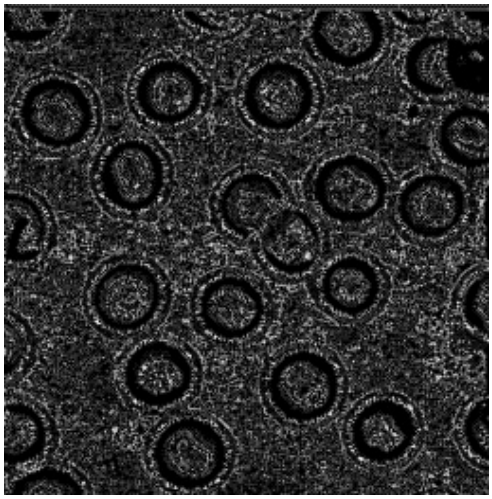

Figure 5: Sampling using Laplacian

6 DISCUSSION

The main result is that the image quality is always very good in the case of the sampling techniques based on the Laplacian: it is difficult to see the differences between the reconstructed image and the original. In the average, the level of gray of a pixel of the reconstructed image and the one of the corresponding pixel of the original image do not differ by more than 1 with the Laplacian based sampling techniques. The alternative Laplacian sampling technique gives very often a smaller maximum error. The best compression ratios are always obtained by the ordinary Laplacian sampling technique. The sampling technique based on the derivative in the direction of the gradient does not give visually satis-

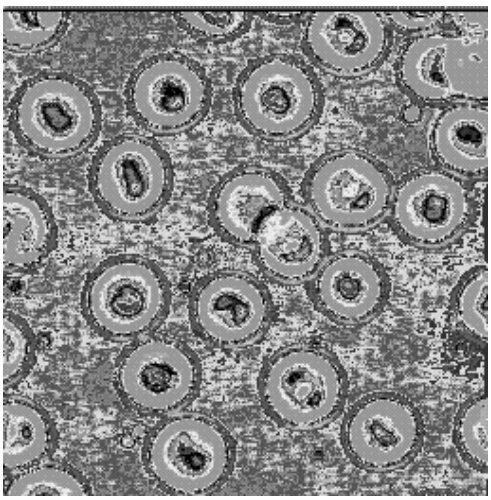

Figure 6: Reconstruction using directional derivative

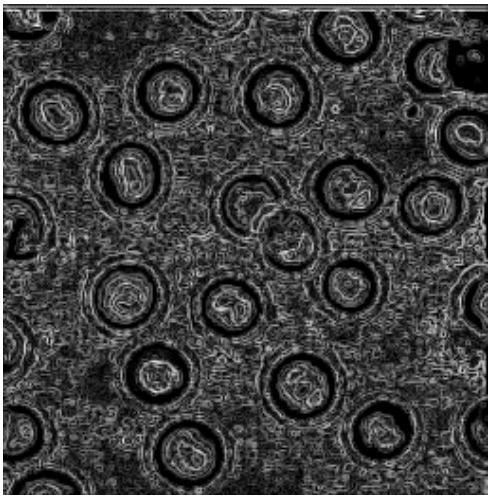

Figure 7: Sampling using directional derivative

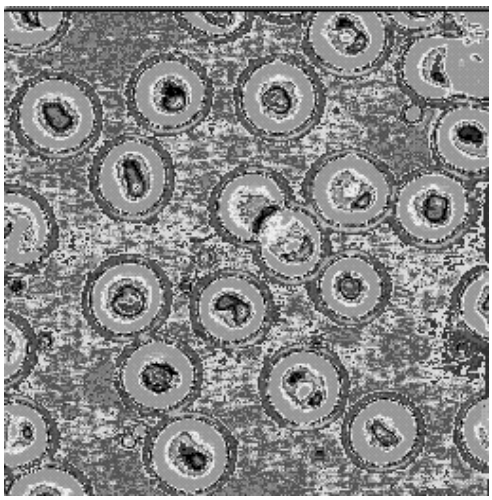

Figure 8: Reconstruction using alternative Laplacian

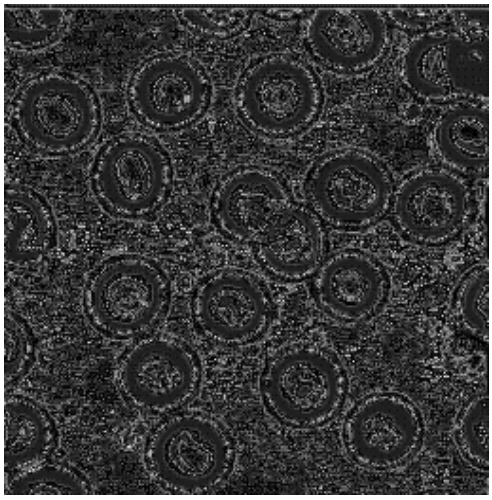

Figure 9: Sampling using alternative Laplacian

fying reconstructed images in all the cases (e.g. the mailbox image, see Table 5 and Figures 16 and 17). However, this reconstruction technique based on natural neighbour interpolation gives reconstructed images of good quality. We feel that this technique is useful when one is presented with irregularly spaced samples, or when one can determine the representative samples oneself, in which case using the standard Laplacian appears to give the best results. In coulour images, an obvious solution is to treat the three colour channels as three independent images to be treated separately. Better results can be obtained using the fact that luminance edges are much better detected by the human visual system than chrominance edges, and therefore one would use a higher threshold on the Laplacian for the chrominance than for the luminance.

7 ACKNOWLEDGMENTS

This research work has received the financial support of the Natural Sciences and Engineering Research Council of Canada (NSERC).

REFERENCES

[Anton98] Anton, F., Gold, C.M., and Mioc, D.: Local coordinates and interpola-

Measures	Lapl.	Grad.	Alt. L.
L_1	0.4525	0.0015	0.0746
L_2	2.0960	0.0402	0.6782
L_∞	197	2	19
Compression	60.6%	0.8%	1.5%

Table 2: Results for goat image (Figure 10)

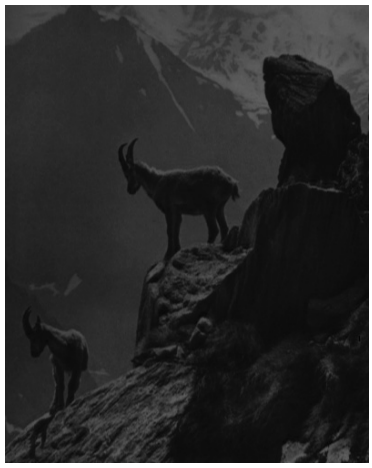

Figure 10: Goat image

tion in a Voronoi diagram for a set of points and line segments, *Voronoi Conference on Analytic Number Theory and Space Tillings*, Kiev, Ukraine, September 1998, pp. 9-12, 1998

[Farin90] Farin G.: Surfaces over Dirichlet tessellations, *Computer Aided Geometric Design* **7** (1-4), pp. 281-292, 1990

[Foley90] Foley, J. D., van Dam, A., Feiner, S. K., and Hughes, J. F.: *Computer Graphics - Principles and Practice, Addison-Wesley*, Reading, Massachussets, 1990

[Gold94] Gold, C.M., and Roos, T.: Surface Modelling with Guaranteed Consistency - An Object-Based Approach, In: J. Nievergelt, T. Roos, H-J. Schek, P. Widmayer (ed.) *IGIS'94: Geographic Information Systems*, Springer, pp. 70-87, 1994

[Guiba85] Guibas, L., and Stolfi, J.: Primitives for the Manipulation of General Subdivisions and the Computation of Voronoi Diagrams, *ACM Transactions*

Measures	Lapl.	Grad.	Alt. L.
L_1	0.1336	0.0026	0.0317
L_2	0.6131	0.0914	0.5670
L_∞	73	6	19
Compression	19.6%	0.4%	0.4%

Table 3: Results for bone marrow image (Figure 12)

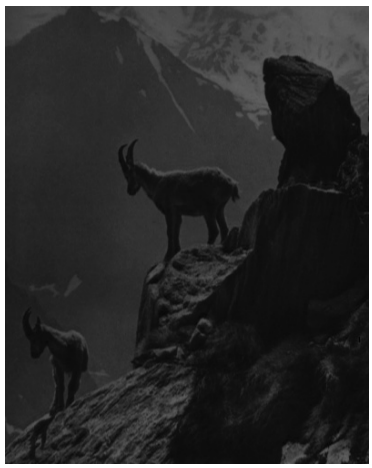

Figure 11: Goat image best reconstruction

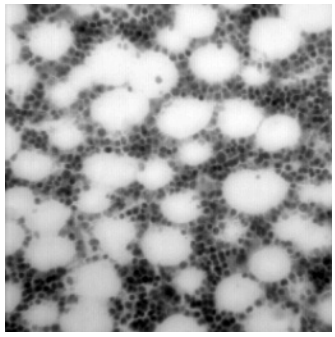

Figure 12: Bone marrow image

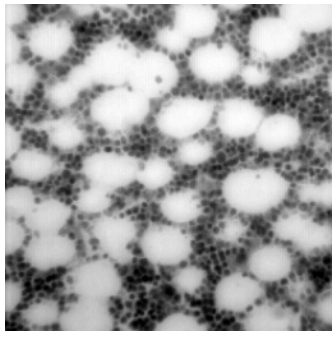

Figure 13: Bone marrow image best reconstruction

Measures	Lapl.	Grad.	Alt. L.
L_1	0.0499	0.2528	0.2130
L_2	1.0797	1.9380	1.8696
L_∞	119	43	58
Compression	35.7%	4.2%	3.6%

Table 4: Results for figure image (Figure 14)

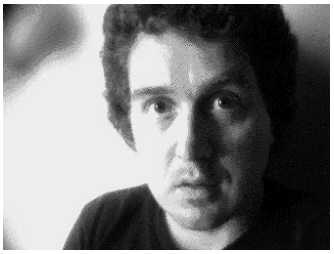

Figure 14: Figure image

on Graphics, Vol. 4, No. 2, pp. 74-123, 1985

[Hinke98] Hinkenjann, A., and Pietrek, G.: Reconstructing Radiosity by Scattered Data Interpolation, *Proceedings of the Sixth International Conference in Central Europe on Computer Graphics and Visualization'98,* University of West Bohemia, Plzen, Czech Republic, Vol. I, pp. 133-140, 1998

[Kuo98] Kuo, M. H., and Chen, M. C.: Biomedical Data Interpolation for 3D visual models, *Proceedings of the Sixth International Conference in Central Europe on Computer Graphics and Visualization'98,* University of West Bohemia, Plzen, Czech Republic, Vol. II, pp. 208-214, 1998.

[Piper93] Piper, B.: Properties of Local Coordinates Based on Dirichlet Tes-

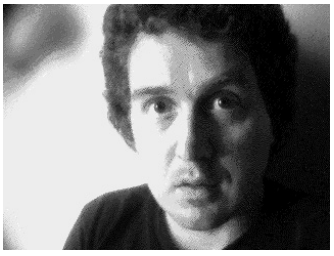

Figure 15: Figure image best reconstruction

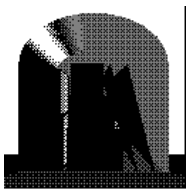

Figure 16: Mailbox image

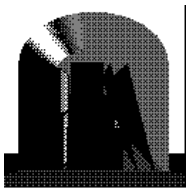

Figure 17: Mailbox image best reconstruction

sellations, *Computing Suppl.*, Vol. 8, Springer, 227-239, 1993

[Ritte96] Ritter, G. X.: *Handbook of Computer Vision Algorithms in Image Algebra*, CRC Press, Boca Raton, Florida, 1996

[Rosen69] Rosenfeld A.: *Picture Processing by Computer*, Academic Press, New York, 1969

[Rosen76] Rosenfeld, A., and Kak A. C.: *Digital Picture Processing*, Academic Press, New York, 1976

[Sibso80] Sibson, R.: A vector identity for the Dirichlet tessellations, *Math. Proc. Cambridge Philos. Soc.*, Vol. 87, pp. 151-155, 1980

[Sibso81] Sibson R.: A brief description of the natural neighbour interpolant, In: D. V. Barnett (ed.) *Interpreting Multivariate Data*, New York, Wiley, 1981

Measures	Lapl.	Grad.	Alt. L.
L_1	0.0392	12.5351	0.0000
L_2	0.2131	38.0251	0.0000
L_∞	12	255	0
Compression	64.6%	50.4%	35.6%

Table 5: Results for mailbox image (Figure 16)